Article

Multicomponent Combinatorial Development and Conformational Analysis of Prolyl Pseudo-Peptide Catalysts: Application in the Direct Asymmetric Michael Addition

Alexander Fernandéz de la Torre, Daniel García Rivera, Marco A. B. Ferreira, Arlene G. Corrêa, and Marcio Weber Paixao

J. Org. Chem., **Just Accepted Manuscript** • DOI: 10.1021/jo401609z • Publication Date (Web): 22 Sep 2013

Multicomponent Combinatorial Development and Conformational Analysis of Prolyl Peptide-Peptoid Hybrid Catalysts: Application in the Direct Asymmetric Michael Addition

Alexander F. de la Torre,[†] Daniel G. Rivera,[†,‡,*] Marco A. B. Ferreira,[†] Arlene G. Corrêa[†] and Márcio W. Paixão[†,*]

[†]Departamento de Química, Universidade Federal de São Carlos, São Carlos, SP, 97105-900, Brazil.

[‡]Center for Natural Products Study, Faculty of Chemistry, University of Havana, Zapata y G, 10400, La Habana, Cuba.

Corresponding Authors *Emails: dgr@fq.uh.cu (D. G. Rivera); mwpaixao@ufscar.br (M. W. Paixão). Tel. and Fax: +55-16-220 8075.

Graphical Abstract

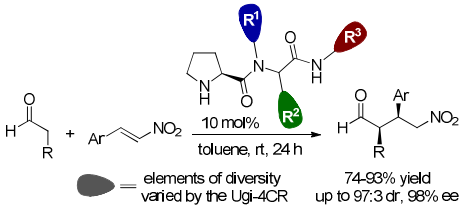

Abstract

A solution-phase combinatorial approach based on the Ugi four-component reaction was implemented for the development of new prolyl peptide-peptoid hybrid catalysts. Three different elements of diversity were varied during the creation of the set of catalysts, i.e., the amine, the oxo and the isocyano components. The multicomponent nature of this process enabled the straightforward generation of a series of peptide-peptoid hybrids having the generic sequences Pro-*N*-R^1-Xaa-NHR^3, being Xaa either Gly (R^2 = H) or Aib (R^2 = *gem*-Me), and R^1 and R^3 either alkyl or amino acid substituents. The catalytic behavior of the peptide-peptoid hybrids was assessed in the asymmetric conjugate addition of aldehydes to nitroolefins, where most catalysts showed great efficacy and rendered the Michael adducts in good to excellent enantio- and diastereoselectivity. A molecular modeling study was performed for two distinct catalysts aiming to understand their conformational features. The conformational analysis provided important information for understanding the remarkable stereocontrol achieved during the organocatalytic transformation.

Keywords: organocatalysis, Michael addition, multicomponent reactions, peptides, combinatorial chemistry, conformational analysis

Introduction

The pursuit of novel chiral molecules for applications in metal-free asymmetric catalysis has inspired intensive research activity in the last decade. This massive effort has resulted in the discovery of several efficient organocatalysts for highly enantio- and diastereoselective organic reactions as well as cascade reaction sequences.[1] Among them, an important class of organocatalysts is that composed of oligopeptidic scaffolds, which have found remarkable applications in a wide range of catalytic asymmetric transformations such us: acylation, oxidation, ester hydrolysis, Aldol reaction, conjugate addition, etc.[2] Although rational design plays an important role in the discovery of organocatalysts, usually further optimization steps including the variation of the nature and position of substituents around the chiral motif are required. In such a lead-catalyst optimization stage, combinatorial chemistry frequently plays a pivotal role owing to its capacity to efficiently produce and screen hundreds of substances in a massive, parallel manner.[3] This strategy has been crucial in peptide catalyst discovery and development,[2,3] mainly due to the great advances in the solid-phase combinatorial synthesis and high-throughput screening of peptide libraries.

However, a different scenario shows up in solution-phase approaches for organocatalyst development, as these latter are less straightforward and thus require a much higher synthetic effort on the preparation of compound libraries for catalytic activity screening. A solution for this may be the utilization of multicomponent reactions (MCRs),[4] i.e., one-pot procedures that incorporate at least three starting materials into a single structure. MCRs are almost unraveling approaches in terms of chemical efficiency, atom economy and diversity generation.[5] Hence, their utilization is of high incidence in drug discovery and development strategies based on the production of hetero- and polycyclic scaffolds, whereas the number of relevant hits can be significantly increased by taking advantage of the diversity-oriented character of such transformations.[6] However, despite the discovery of new catalysts can be

approached in a similar way as drug discovery, the interest of the catalysis community in MCRs does not yet reflect the proven impact of such processes in other important areas like medicinal[6] and natural products chemistry.[7]

Among the different types of peptide catalysts, those having proline at the *N*-terminus are especially suitable for both enamine and iminium ion activation. In a series of recent reports, Wennemers and co-workers used a combination of rational design and combinatorial chemistry for the development of tripeptides based on the generic structure Pro-Pro-Xaa (Xaa being an acidic α-amino acid).[8] Thus, the so-called Wennemers catalyst D-Pro-Pro-Glu-NH_2 (Fig. 1A) has been recognized as one of the most effective for the asymmetric conjugate addition of aldehydes to nitroolefins, while other analogs have been also developed for the catalytic asymmetric Aldol reaction.[9]

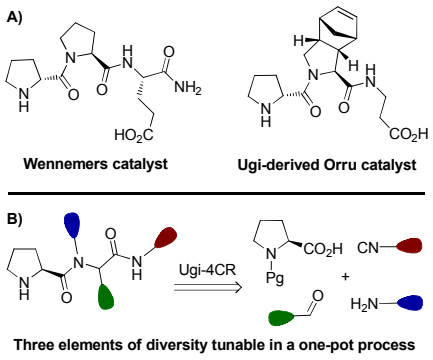

Figure 1. A) Prolyl peptide catalysts for asymmetric conjugate additions. B) Combinatorial multicomponent strategy for the preparation of prolyl peptide-peptoid hybrids.

Perhaps the MCR of greater promise in the field of peptide catalysis is the Ugi four-component reaction (Ugi-4CR).[10] This reaction has proven to be a powerful tool for the efficient preparation of peptidic skeletons, including *N*-alkylated peptides and a wide variety of peptidomimetic.[3,11] Recently, Orru and co-workers implemented a highly diastereoselective Ugi reaction for the straightforward synthesis of a prolyl peptide[12] (Fig. 1A) resembling the

structure and catalytic behavior of Wennemers catalyst, which proved the potential of such a reaction for accessing target peptides.

Herein we report the application of the Ugi-4CR for the combinatorial development of novel peptide-peptoid hybrid catalysts as well as the assessment of their catalytic behavior in the asymmetric conjugate addition of aldehydes to nitroolefins. As depicted in figure 1B, our strategy focuses on exploiting the diversity-generating capability of this reaction in the solution-phase production of a collection of compounds integrating structural elements of peptides and peptoids (in *sensu strictu* peptoids are defined as *N*-substituted polyglycines). Thus, this approach differs from that of Orru *et al.*[12] in the sense that the use of the MCR does not aim the synthesis of a target peptide catalyst, but a collection of them for addressing the effect of the structural variations on the catalytic profile.

Results and Discussion

Solution-Phase Multicomponent Synthesis of Prolyl Peptide-Peptoid Hybrid Catalysts. The classic Ugi-4CR[10] is the one-pot condensation of a primary amine, an oxo compound (i.e., ketone or aldehyde), a carboxylic acid, and an isocyanide to produce an *N*-substituted dipeptide backbone, which may be considered as a peptide-peptoid hybrid[13] when α-amino acids are used either as carboxylic or amino components. As early proposed by Ugi himself, the multicomponent nature of this process enables the development of powerful combinatorial procedures through variation of each of the four starting materials. Whereas this concept has been previously applied in drug discovery,[6] we are not aware of its implementation in organocatalysts discovery.[14] As illustrated in figure 1B, we planned the installation of three elements of tunable diversity, i.e., the amine, the oxo and the isocyanide components, while proline remains as a fixed substrate aiming to enable enamine catalysis. As a result, the simple variation of highly available substrates like primary amines, carbonyl compounds and

isocyanides may give rise to a medium-size library of structurally novel prolyl peptide-peptoid hybrids for screening of their catalytic behavior.

As shown in table 1, the implementation of the multicomponent combinatorial approach required a two-step procedure comprising the one-pot assembly of the peptidic skeleton by the Ugi-4CR followed by *N*-terminus deprotection. Among the three distinct elements of diversity, initial attention was posed on the variation of the amine (entries 1-8), while paraformaldehyde and cyclohexylisocyanide were kept as fixed components. A typical Ugi protocol[10b] was implemented for all catalysts in a first instance, which proved to be suitable for reactive amines (entries 1, 7-12) but gave poor results when sterically congested α-amino acid methyl esters were used (entries 2-6).

Table 1. Multicomponent combinatorial synthesis of prolyl peptide-peptoid hybrid catalysts using the Ugi-4CR either at room temperature or under microwave irradiation.

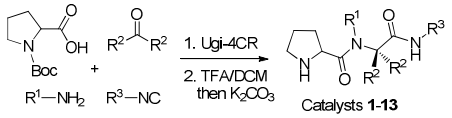

Entry	Acid	R^1	R^2	R^3	Catalyst	Yield[c]
1	L-Pro	Gly-OMe[a]	H	Cy	**1**	78%
2	L-Pro	Val-OMe[b]	H	Cy	**2**	81%
3	L-Pro	Leu-OMe[b]	H	Cy	**3**	85%
4	L-Pro	Ile-OMe[b]	H	Cy	**4**	77%
5	L-Pro	Phe-OMe[b]	H	Cy	**5**	83%
6	L-Pro	^{t}BuGly-OMe[b]	H	Cy	**6**	61%
7	L-Pro	(*S*)-α-MeBn[a]	H	Cy	**7**	91%
8	L-Pro	Bn[a]	H	Cy	**8**	93%
9	L-Pro	(*S*)-α-MeBn[a]	Me	Cy	**9**	77%
10	L-Pro	Bn[a]	Me	Cy	**10**	73%
11	L-Pro	(*S*)-α-MeBn[a]	H	*t*-Bu	**11**	88%
12	L-Pro	(*S*)-α-MeBn[a]	H	Gly-OMe	**12**	82%
13	D-Pro	(*S*)-α-MeBn[a]	Me	Cy	**13**	79%

[a]Reaction conducted at room temperature in MeOH for 24h. [b]Reaction conducted under microwave irradiation. [c]Yield of isolated pure product over two steps.

The solution for this was the use of microwave irradiation, which comprised good efficiency in the multicomponent preparation of the catalysts **2**-**6**, whereas up to three cycles (30 min, 150 W, 70 °C) of irradiation were required in the reaction of the unreactive L-*t*-butylglycine methyl ester (entry 6). We next looked onto the variation of the oxo and isocyano components, again relying on the use of readily available starting materials to produce accessible catalysts. Thus, acetone was utilized as oxo component in combination with both (*S*)-α-methylbenzyl and benzyl amines (entries 9 and 10), leading to catalysts **9** and **10** having the secuence Pro-*N*-alkyl-Aib (Aib is α-aminoisobutyric acid). Alternatively, *t*-butylisocyanide and methyl isocyanoacetate were combined with (*S*)-α-methylbenzylamine and paraformaldehyde (entries 11 and 12) to produce the catalysts **11** and **12**. In a last instance, (*S*)-α-methylbenzyl amine, acetone and cyclohexylisocyanide were combined with D-Pro to produce catalyst **13**, an analog of **9** having the opposite stereochemistry at proline. With this we might be able to assess the actual role of the pyrrolidine-ring stereochemistry on the sterecocontrol performed by such catalysts. Alternatively, with the change of the amino and isocyano components we aimed to address the influence on the catalytic profile of the bulky character of substituents at both the internal and *C*-terminal amides. On the other hand, the variation of *N*-alkyl-Gly by *N*-alkyl-Aib – derived from the change of formaldehyde by acetone, respectively – aims to address the influence of the peptide conformational flexibility in the catalytic performance. It must be noticed that the utilization of prochiral aldehydes and ketones is certainly possible in this combinatorial protocol, whereas this initial report skips the difficulty associated with the separation and identification of the resulting diastereomers.

Assessment of the enamine-type catalytic performance

With the library of peptide-peptoid hybrid catalysts in hand, we turned to the evaluation of their organocatalytic performance in the Michael addition. This class of chemical transformation is recognized as one of the most powerful C-C bond-forming reactions,[15] and –

since the discovery of its aminocatalytic version[16] – it has been traditionally selected for assessing the potential of new catalysts acting through enamine catalysis.[1] Important insights into the mechanism of the catalytic conjugate addition of aldehydes to nitroolefins have been reported in recent years[17] with the use of the diphenylprolinol silyl ether, one of the most effective catalysts in the stereoselective version of this process.[18] To screen the performance of peptide-peptoid hybrids **1**-**12**, their catalytic efficiency and stereoselection were initially assessed in the model system consisting in the conjugate addition of *n*-butanal to *trans*-*β*-nitrostyrene. During the initial screening, standard reaction conditions consisting in the use of 10 mol% of catalyst in toluene as solvent at room temperature were chosen.

Table 2. Screening of the enamine-catalytic performance of peptide-peptoid hybrids **1**-**12** in the asymmetric Michael addition.

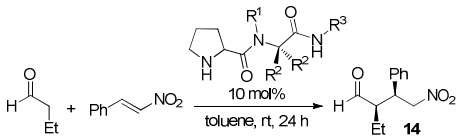

Entry	Acid/R^1/R^2/R^3	Yield (%)[b]	dr (*syn*/*anti*)[c]	ee (%)[d]
1	L-Pro/Gly-OMe/H/Cy (**1**)	87	96:4	90
2	L-Pro/Val-OMe/H/Cy (**2**)	92	92:8	91
3	L-Pro/Leu-OMe/H/Cy (**3**)	83	97:3	79
4	L-Pro/Ile-OMe/H/Cy (**4**)	89	97:3	90
5	L-Pro/Phe-OMe/H/Cy (**5**)	84	93:7	64
6	L-Pro/^{t}BuGly-OMe/H/Cy (**6**)	94	90:10	82
7	L-Pro/MeBn/H/Cy (**7**)	74	96:4	89
8	L-Pro/Bn/H/Cy (**8**)	91	93:7	92
9	L-Pro/MeBn/Me/Cy (**9**)	85	94:6	98
10	L-Pro/Bn/Me/Cy (**10**)	84	94:6	87
11	L-Pro/MeBn/H/*t*-Bu (**11**)	93	94:6	91
12	L-Pro/MeBn/H/Gly-OMe (**12**)	77	89:11	85
13	D-Pro/MeBn/Me/Cy (**13**)	93	84:16	-86

[a]All reactions were conducted, using 3 equivalents of the aldehyde. [b]Yield of isolated product as mixture of *syn*/*anti* adducts. [c]Determined by ^{1}H NMR spectroscopy (of the crude mixture) and HPLC analysis. [d]Determined by chiral stationary phase HPLC analysis on the major diastereomer.

As illustrated in table 2, most compounds catalyzed the Michael addition with good to excellent enantio- and diastereoselectivity, showing catalysts **9** the best results in terms of

stereocontrol (98% ee, 94:6 dr). Analysis of these results provides important insights into the structural requirements (derived from the three elements of diversity) for this new class of catalysts to be effective. Thus, in terms of chemical efficiency and diastereoselection, it does not seem to be great differences between all catalysts, whereas the enantioselection resulted more dependent on some of the variable structural elements. Among these tunable structural elements, variation of the chirality and bulky character of the *N*-substituent derived from the amino component (entries 1-8, table 2) did not lead to a clear tendency in the enantioselectivity behavior when formaldehyde was employed as the oxo component. As depicted in table 2, the presence of the achiral *N*-substituents Gly-OMe (entry 1) and benzylamine (entry 8) provided similar results (i.e., *ca.* 90% ee) that the chiral ones Val-OMe (entry 2), Ile-OMe (entry 4) and (*S*)-α-methylbenzylamine (entry 7). Alternatively, Val-OMe (entry 2) and Ile-OMe (entry 4) showed much better enantioselectivity than Leu-OMe (entry 3) and Phe-OMe (entry 5), but – intriguingly – L-*t*BuGly (entry 6) gave only moderate results despite of having the bulkiest side chain among all aminoacid methyl esters incorporated as *N*-substituents.

On the other hand, the incorporation of the aminoacid residue Aib – derived from the use of acetone instead of formaldehyde as oxo component – shed additional light into the structure catalytic-activity relationship. Thus, the combination of Aib (R^2 = Me) and the chiral (*S*)-α-methylbenzyl group as *N*-substituent led to the most effective catalyst **9** (98% ee, entry 9). Intriguingly, catalyst **10** bearing benzyl as *N*-substitution exhibited only moderate enantioselectivity (entry 10), despite of also having the aminoacid residue Aib (R^2 = Me) derived from the use of acetone in the Ugi-4CR.

We next looked into the effect of varying the isocyanide component in the stereocontrol of the conjugate addition, while keeping the oxo and amino components fixed (i.e.; R^1 = (*S*)-α-MeBn and R^2 = H). Thus, catalysts **11** (entry 11, R^3 = ^{t}Bu) showed slightly higher

enantioselectivity than its analogue **7** (entry 7, R^3 = Cy), probably due to bulkier character of the *t*-butyl amide substituent compared to the cyclohexyl one. In contrast, the incorporation of the less bulky methyl isocyanoacetate in catalyst **12** (entry 12, R^3 = Gly-OMe) led to a drop in both the enantio- and diastereoselectivity with respect to catalyst **7**. Based on these results, it can be stated that the incorporation of an isocyanide component with certain steric hindrance is important, although there are no great differences between catalysts having the terminal *t*-butyl and cyclohexyl carboxamides. Thus, the use of cyclohexylisocyanide becomes more feasible than the *t*-butyl one owing to the lower price and simpler synthesis of the former.

Finally, catalyst **13** provided good enantio- and diastereoselectivity while producing the Michael adduct with the reversed configuration at the asymmetric centers (entry 13), thus proving that the stereocontrol is mainly biased by the pyrrolidine-ring stereochemistry. Nevertheless, in this case the topological matching with the (*S*)-α-methylbenzyl *N*-substituent is less effective than for catalyst **9** based on L-Pro, as the enantioselection of the latter was significantly higher.

At this stage, we anticipated that the increased conformational rigidity provided by the incorporation of both the aminoacid Aib instead of Gly (e.g., comparison of **9** with **7**) and the chiral *N*-substituent (*S*)-α-MeBn instead of Bn (e.g., comparison of **9** with **10**) is the crucial factor in the higher enantioselectivity of catalyst **9** compared with its congeners. Such a greater conformational rigidity of **9** – derived from both the geminal methyl groups and the chiral *N*-substituent – was confirmed by NMR analysis. Thus, duplicate sets of signals was observed in the NMR spectra of most catalysts – due to the presence of the *cis* and *trans* isomers of the *N*-substituted amide bond.[19] However, the ^{1}H NMR spectrum of catalyst **9** showed a single configurational isomer in solution, thus confirming the conformational fixation effect provided by its key structural elements.

Indeed, the above findings were only possible due to the multicomponent nature of the combinatorial procedure, in which three elements of diversity can be parallelly varied keeping L-proline as a fixed component. Whereas it was proven that slight structural variations may allow for a fine tuning of the enantioselectivity, we were prompted to the preparation of peptide-peptoid hybrid catalysts including Aib in the backbone and aminoacid methyl esters as *N*-substituents instead of aliphatic amines. Unfortunately, the yields of such Ugi-4CRs were rather poor – even with the utilization of microwave irradiation – presumably due to the inefficient imine formation starting from acetone and aminoacid methyl ester hydrochlorides in presence of 1 equivalent of Et_3N.

Table 3. Substrate scope of the asymmetric Michael addition of aldehydes to *trans*-β-nitrostyrenes catalyzed by peptide-peptoid hybrid **9**.

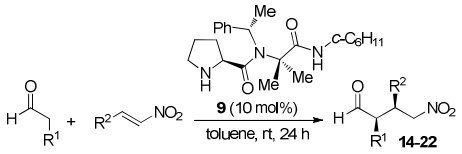

Entry	R^1	R^2	Compound	Yield (%)[b]	dr (*syn*/*anti*)[c]	ee (%)[d]
1	Et	Ph	14	85	94:6	98
2	*i*-Pr	Ph	15	81	91:9	67
3	Et	4-$MeOC_6H_4$	16	83	82:18	93
4	Et	4-FC_6H_4	17	89	92:8	96
5	Et	4-ClC_6H_4	18	86	94:6	88
6	Et	4-BrC_6H_4	19	84	86:14	86
7	Et	2-BrC_6H_4	20	91	88:12	89
8	Et	3-$NO_2C_6H_4$	21	70	81:19	78
9	Et	2-Furyl	22	83	93:7	82

[a]All reactions were conducted using 3 equivalents of the aldehyde. [b]Yield of isolated product as mixture of *syn*/*anti* adducts. [c]Determined by ^1H NMR spectroscopic. [d]Determined by chiral-phase HPLC analysis on the major diastereomer.

By analysis of table 2, peptide-peptoid hybrid **9** proved to be the most effective one in the initial reaction conditions. Therefore, we next turned to assess the substrate scope of the conjugate addition catalyzed by organocatalyst **9.** As depicted in table 3, a variety of substituted *trans*-*β*-nitrostyrenes were utilized to afford the Michael adduct in good to

excellent enantioselectivity, albeit in some cases only with moderate diastereoselectivity. Utilization either of *trans*-2-furyl-nitroolefin as acceptor (entry 9) or isovaleraldehyde as donor (entry 2) provided Michael adducts in high diastereoselectivity but only moderate enantioselectivity.

To assess the effect of reaction conditions in the catalytic efficiency and stereocontrol of this type of catalysts, a variety of solvents, conditions and additives were studied. As shown in table 4, catalyst **2** was initially chosen to accomplish this study considering that its performance in the model system was high (entry 1) but yet improvable. In this sense, catalyst **9** was not selected for this purpose owing to the fact that its enantioselection was already quite high, and thereby difficult to improve through variation of conditions. Thus, neither decreasing the temperature to 5 ºC (entry 1) nor adding 10 mol% of either benzoic acid (entry 3) or *p*-nitrophenol (entry 4) provoked a significant change in the reaction yield and stereoselection. In the case of *p*-nitrophenol as additive, a qualitative study revealed an initial acceleration of the reaction, although the yield was not increased after 24 h. Alternatively, decreasing the catalyst loading to 5 mol% (entry 5) and 2.5 mol% led to an erosion in the reaction yield, albeit the enantio- and diastereoselectivity remained high. The solvent change also decreased the effectiveness of the catalyst, especially when very polar solvents were employed. Hence, either DCM or mixtures containing a small amount of *i*-PrOH (entries 8 and 9) were less successful than pure toluene, while both pure *i*-PrOH and THF provoked an improvement in the reaction yield but a marked drop of the enantio- and diastereoselection. Whereas this proves that non-protic, hydrophobic solvents are required for a good stereocontrol, the results are quite intriguing since the mixture $CHCl_3$/*i*-PrOH is the solvent of choice for Michael additions with Wennemers' peptide catalysts.[8]

Table 4. Effect of reaction conditions on the asymmetric Michael addition catalyzed by peptide-peptoid hybrids **2** and **3.**

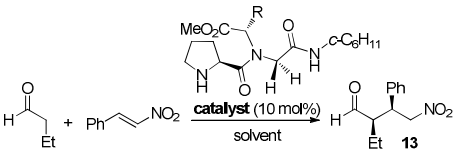

Entry	Catalyst	Solvent	mol%	Yield (%)[b]	dr (*syn*/*anti*)[c]	ee (%)[d]
1	2	PhMe	10	92	92:8	91
2	2	PhMe[e]	10	89	95:5	90
3	2	PhMe[f]	10	88	94:6	87
4	2	PhMe[g]	10	92	93:7	90
5	2	PhMe	5	76	94:6	89
6	2	PhMe	2.5	45	96:4	91
7	2	DCM	10	74	94:6	79
8	2	PhMe/*i*-PrOH[h]	10	90	95:5	80
9	2	CH_3Cl/*i*-PrOH[h]	10	63	93:7	62
10	2	*i*-PrOH	10	98	85:15	34
11	2	THF	10	98	88:12	73
12	3	PhMe	10	83	68:32	79
13	3	PhMe[f]	10	57	94:6	49
14	3	CH_3Cl/*i*-PrOH[h]	10	61	94:6	47
15	3	THF	10	91	90:10	64

[a]Reactions were conducted using 3 equivalents of the aldehyde, and unless otherwise specified, at room temperature for 24 h. [b]Yield of isolated product as mixture of *syn*/*anti* adducts. [c]Determined by ^{1}H NMR spectroscopic (of the crude mixture) and HPLC analysis. [d]Determined by chiral-stationary phase HPLC analysis on the major diastereomer. [e]Reaction conducted at 5 ºC. [f]10 mol% of benzoic acid was used as additive. [g]10 mol% of *p*-nitrofenol was used as additive. [h]Solvent mixture 9:1 (*v*/*v*).

As illustrated in table 4, we also decided to evaluate catalyst **3** in a variety of conditions, considering that the effectiveness of this catalyst might be yet improvable. However, neither the presence of an acid additive (entry 13) nor the utilization of more polar solvents like $CHCl_3$/*i*-PrOH (entry 14) and THF (entry 15) led to higher enantio- and diastereoselectivity compared to the original conditions (entry 12).

For catalysts derived from L-proline, the absolute configuration of Michael adducts was unambiguously established to be 2*R*,3*S* according to chemical correlation with previous reports (see the Experimental Part). This enantioselection can be explained according to the Seebach's topological model,[20] in which the *anti* enamine approaches to the nitroolefin by the

less hindered face through a synclinal transition state. To understand the enantioselectivity observed in this work, the peptidic substituent at the pyrrolidine ring must favor the formation of the enamine with the *E* configuration while providing an important shielding to the *Re*-face. Accordingly, we were prompted to undertake a conformational study aimed at understanding both the actual shielding effect to one of the pyrrolidine (and therefore enamine) faces and the dissimilar *cis-trans* isomerizations detected by NMR in catalysts incorporating either *N*-substituted Gly or Aib.

Conformational Analysis

A conformational analysis was accomplished for the parent catalysts **7** and **9**, keeping in mind that: *i*) the sterocontrol provided by **9** was higher that of **7** and *ii*) NMR analysis of **9** shows almost a single configurational isomer while that of **7** shows a mixture of *cis* and *trans* isomers in solution (see NMR spectra in the Supporting Information A).

To cover the conformational space of catalyst **7**, we initially conducted a conformational search by Monte Carlo Molecular Mechanics (MCMM) as implemented in Macromodel 9.9. We were able to find 673 different conformers with energies within 5 kcal.mol^{-1} relative to the lowest-energy conformation. Clustering according to the atomic distances of heavy-atoms eliminated the redundant conformers, resulted in 42 groups (see in the Supporting Information B). The same conformational search was performed with catalyst **9**, resulting in 182 different conformers and 26 groups after clustering analysis. Representative structures of low-energy clustered conformers were selected and re-optimized at M06-2X/6-31G(d). The electronic energies were refined by a single point using the 6-31+G(d,p) basis set. The relative Gibbs energies and Boltzmann population at 25 ºC in $CDCl_3$ of all re-optimized low-energy conformers are shown in supporting information B (see Tables S1, S2, S3, and S4).

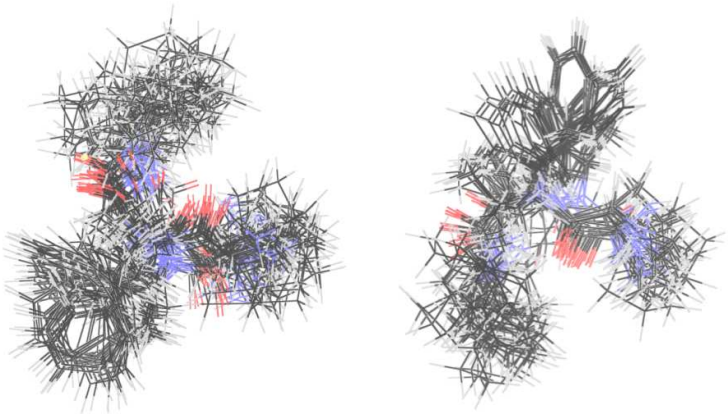

Catalyst 7 **Catalyst 9**

Figure 2. Low-energy clustered-superposed conformers of catalysts **7** and **9** calculated at M06-2X/6-31+G(d,p) // M06-2X/6-31G(d) [SDM, chloroform] level.

As shown in Figure 2, analysis of superposed geometries of these re-optimized low-energy conformers indicated that a restricted conformational space was adopted by the conformers. Nevertheless, it is evident that the conformational rigidity of catalyst **9** is higher than that of **7**, which confirms the NMR behavior of both catalysts. The notation used to represent the conformations of catalysts **7** and **9** was focused on the plane through the tertiary amide bond. As can be seen in the graphical representation of Table 5, the Ph- and NH-cyclohexyl groups were selected to define either the positive (+) or negative (-) orientation of the dihedrals Ψ_1 and Ψ_2 (see in Tables S2 and S4 of SI-B the assignment in each conformer of this notation). After examination of dihedral orientation of the different conformers of catalysts **7** (Table 5), a ratio of 42:58 of *cis*/*trans* isomers was determined. In contrast, conformational analysis of catalyst **9** revealed an inversion in the equilibrium – with a ratio of 98:2 of *cis*/*trans* isomers – as well as a marked difference in the orientations of the dihedrals compared to catalyst **7**.

Table 5. Graphical representation and excerpt of dihedral distribution for catalysts **7** and **9**.

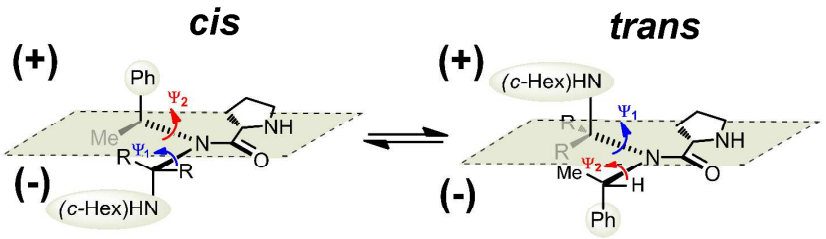

		Ψ1(+)/Ψ2(-)	Ψ1(-)/Ψ2(+)	Ψ1(+)/Ψ2(+)	Ψ1(-)/Ψ2(-)
Cat 7 (R = H)	***cis***	0.1	39.2	2.6	0.0
	trans	42.0	0.0	0.7	15.2
Cat 9 (R = Me)	***cis***	17.3	9.9	17.3	53.6
	trans	0.0	0.0	0.0	1.9

The fact that *cis*-conformers of **9** (R = Me) are lower in energy – and thus most populated – than those of catalyst **7** (R = H), seems to be a crucial factor to understand the difference in the enantioselectivities. As depicted in figure 2, partial shielding to one of the pyrrolidine-ring faces is observed in the low-energy clustered conformers of both **7** and **9**, albeit this is indeed more marked in the case of catalyst **9** that is populated in 98% with *cis*-conformers. To further confirm these results experimentally, two NOESY spectra were recorded for catalyst **9** in $CDCl_3$ in order to determine the disposition of the peptidic chain with respect to the pyrrolidine faces (see the Supporting Information A). Initially, a NOESY spectrum with irradiation of the C*H* signal of the methylbenzyl *N*-substituent at 5.11 ppm showed NOE effects with one of the methylene *β*-protons of proline, which proves the *cis* configuration proposed by molecular modeling. Alternatively, a second NOESY experiment was accomplished with irradiation of the signal (N*H*) of the cyclohexylamide at 5.74 ppm, resulting in NOE effects with protons of the cyclohexyl ring, with the *ortho* protons of the phenyl ring, with one of the *gem*-dimethyl groups of the Aib residue and with a **β**-proton of proline. However, the lack of NOE effect of the α-proton proline at 4.30 ppm – positioned at the non-substituted pyrrolidine face – is a clear indication that the peptidic skeleton is located

directing to the substituted pyrrolidine face. This fully agrees with the *cis*-isomer structures of catalyst **9** shown in figure 2, 3 and 5, wherein the terminal cyclohexyl moiety is positioned at the opposed face of the proline α-proton, thus setting free the non-substituted face upon the enamine formation and further addition to the Michael acceptor. Indeed, such a shielding effect over a specific pyrrolidine face is biased by the proline stereochemistry, and it is hypothesized to be reversed in a catalyst having the opposite configuration at the proline and methylbenzyl stereocenters.

To assess whether the blocking of one of the pyrrolidine faces remains upon enamine formation, a conformational search was performed for the *anti* enamine derived from catalyst **9** and the aliphatic aldehyde. As shown in figure 3, the optimized lowest-energy structure of the enamine with *E* configuration shows a significant shielding of the peptidic skeleton to the *Re*-face, which according to the Seebach's topological model explains the high enantioselection provided by catalyst **9**.

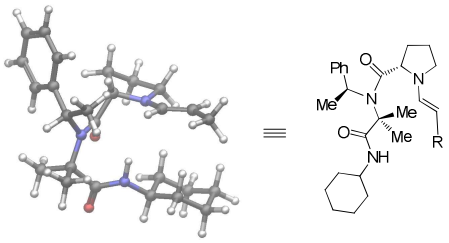

Figure 3. Lowest-energy structure of the *anti* enamine derived from catalyst **9**.

As shown in figure 4, conformational analysis of **7** shed additional light into the *cis-trans* isomerization. We detected that the most populated *trans*-conformers of **7** were the Ψ_1-dihedral rotamers 11-*trans* (38%) and 36-*trans* (13%). Another significant feature was the relative orientation of dihedrals Ψ_1 and Ψ_2. Thus, *cis*-conformers of **7** adopt a Ψ1(-)/Ψ2(+) orientation and *trans*-conformers a Ψ1(+)/Ψ2(-), with both the Ph and *N*-cyclohexyl groups positioned in an opposite direction. We also noticed a persistent hydrogen bonding (HB)

between the oxygen lone pairs $LP_{O(1\ and\ 2)}$ of the tertiary amide carbonyl group and the pyrrolidine σ^*_{N-H} group (NH--O=C) in a wide set of conformers of catalyst **7** (see S1 section in Supporting Information B). In addition, we investigated the transition states TS-1 that represents the *cis*-*trans* equilibration from the more populated 11-*trans* (31%) to 20-*cis* (26%) conformers. The result was an activation energy of 21 kcal/mol, which explains the detection of both configurational isomers of catalyst **7** in the NMR time-scale. The natural bond orbital (NBO) analysis of selected structures 36-*trans*, 11-*trans*, TS-1 and 20-*cis* showed delocalization energies in the range from 1.64 to 4.57 kcal.mol^{-1}. The geometries, Boltzmann population, and Gibbs energies of conformers involving the main *cis*-*trans* isomerization of catalyst **7** are also represented in Figure 4.

Interestingly, an additional stabilizing intramolecular seven-membered rings hydrogen-bonded was detected, which involves the same $LP_{O(1\ and\ 2)}$ and the amide σ^*_{N-H} group (CONH--O=C) of the more hindered 20-*cis* conformer, with energy of 6.12 kcal.mol^{-1} (see Supporting Information B). This explains the slightly higher stability of the lowest-energy 11-*trans* isomer compared with 20-*cis*. Although such a hydrogen bonding may be relevant for this analysis only in the ground state of the catalyst, it must be noted that is even preserved in the TS-1, comprising a high stabilization energy of 11.55 kcal.mol^{-1}.

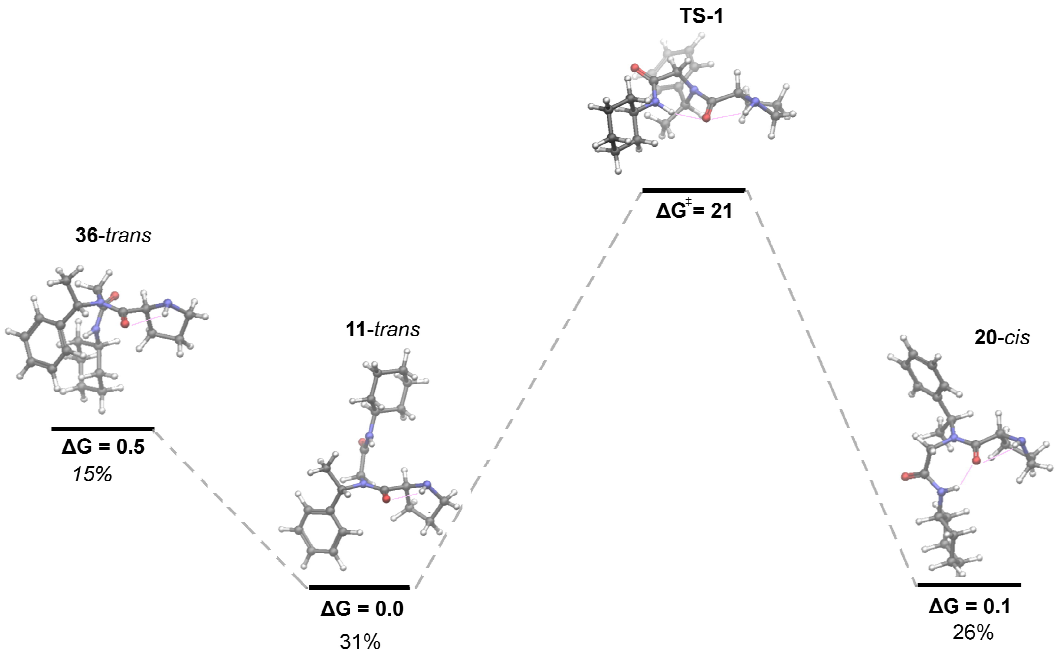

Figure 4. Relevant low-Gibbs energy *cis-trans* conformers and transition state of catalyst **7** at M06-2X/6-31+G(d,p)//M06-2X/6-31G(d) [SDM, chloroform] level.

As depicted in figure 5, conformational analysis of catalyst **9** revealed that 1-*trans* (2%) and the lowest-energy 26-*cis* (33%) conformers adopted a Ψ1(-)/Ψ2(-) orientation, directing axially (according to the imaginary plane of the tertiary amide carbonyl) to the methyl group of (*S*)-α-MeBn *N*-substituent. This orientation is directed by steric clashes involving the equatorial *N*-alkyl H ⇔ Me interaction presented in 1-*trans*, while the Me ⇔ Me interaction increases the energy of 17-*cis* (8%) – a Ψ_1 dihedral-rotamer of **26**-*cis* (Figure 3) – in 1 kcal.mol^{-1}. Similarly to catalyst **7**, it was observed for **9** a persistent hydrogen bonding involving the pyrrolidine σ^*_{N-H} group (NH--O=C) (see S2 section in the SI). NBO analysis of structures 1-*trans* and its rotamer (not located by MM conformational search and drawn manually), as well as **17**-*cis*, **26**-*cis*, and TS-2, showed delocalization energies in the range of 1.68 to 4.59 kcal.mol^{-1}. Interestingly, the located transition state TS-2 comprises an activation energy of 15 kcal.mol^{-1} (6 kcal.mol^{-1} lower in energy than that observed for catalyst **7**), which allows for a relatively fast shift of the equilibrium to the less energetic *cis* isomer.

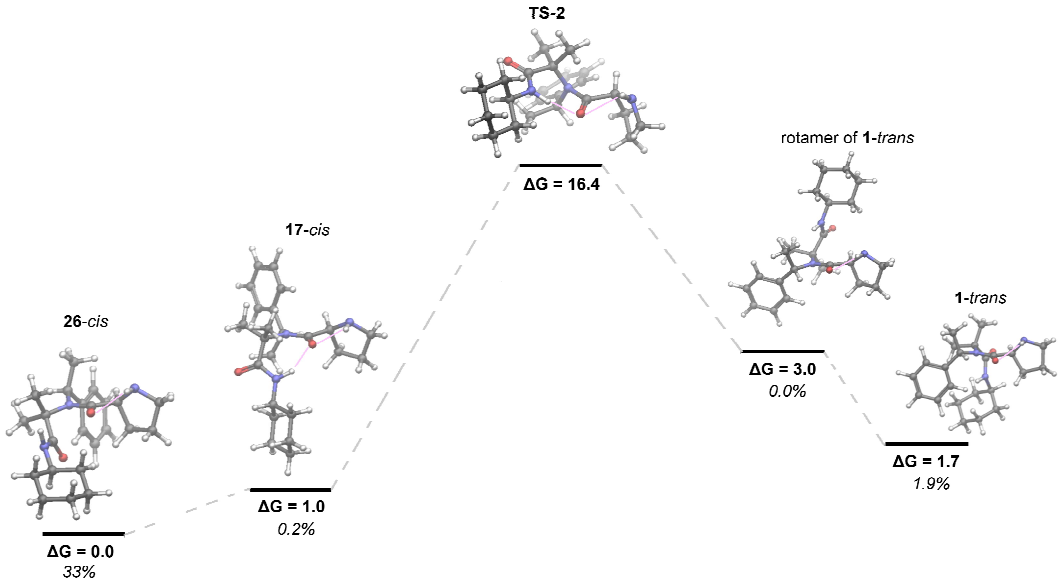

Figure 5. Relevant low-Gibbs energy *cis-trans* amide conformers and transition state of catalyst **9** at M06-2X/6-31+G(d,p) // M06-2X/6-31G(d) [SDM, chloroform] level.

The additional intramolecular hydrogen-bonded seven-membered ring (CONH--O=C) was absented in the lowest-energy conformer 26-*cis*, but it was founded in the 17-*cis* conformer (8.26 kcal.mol^{-1}) and in the TS-2 (13.76 kcal.mol^{-1}) as well. Unexpectedly, the TS-2 leads to a shorten HB than TS-1 (1.886 Å and 1.952 Å, respectively), thus reflecting the crowed transition structure. The geometries, Boltzmann population, and Gibbs energies of these representative structures are represented in figure 5.

Conclusion

This study showed that solution-phase combinatorial approaches based on isocyanide-based MCRs are convenient tools for the discovery of organocatalysts for asymmetric organic transformations. We have illustrated this by the Ugi-4CR-based generation of a small combinatorial collection of new prolyl peptide-peptoid hybrids and the screening of their catalytic efficacy in the asymmetric conjugate addition of aldehydes to nitroolefins. Thus, variation of three elements of diversity at the Ugi-derived *N*-substituted peptide led to the discovery of catalysts providing good to excellent stereocontrol and catalytic efficacy, while

provided new insights into their structure catalytic-activity relationship. A conformational study explained the greater conformational rigidity and stereoselection provided by catalyst **9**, bearing the *N*-substituted amino acid Aib as *C*-terminal residue, compared to **7** that has Gly at the same position. Considering the diversity-oriented character of MCRs, further exploitation of this capacity in the combinatorial discovery of catalysts is foreseeable.

Experimental Section

General

Melting points are uncorrected. ^{1}H NMR and ^{13}C NMR spectra were recorded at 400 MHz for ^{1}H and 100 MHz for ^{13}C, respectively. Chemical shifts (δ) are reported in parts per million relative to tetramethylsilane (TMS), and coupling constants (*J*) are reported in hertz. High resolution ESI mass spectra were obtained from a Fourier transform ion cyclotron resonance (FT-ICR) mass spectrometer, an RF-only hexapole ion guide and an external electrospray ion source. Flash column chromatography was carried out using silica gel 60 (230-400 mesh) and analytical thin layer chromatography (TLC) was performed using silica gel aluminum sheets. HPLC chromatograms were obtained on an apparatus with a LC-10AT Pump, SPD-10A UV-Vis Detector, SCL-10A System Controller, using a Chiralpak AD-H (4,6 mmØ × 250 mmL, particle size 5 μm). Optical rotations were measured with a Polarimeter at 589 nm, 30 °C.

General Ugi-4CR-based procedure: A suspension of the amine (1.0 mmol) and the aldehyde (or ketone) (1.0 mmol) in MeOH (5 mL) was stirred for 1 h at room temperature. NEt_3 (1.0 mmol) was added when α-amino acid methyl ester hydrochlorides were employed. The carboxylic acid (1.0 mmol) and the isocyanide (1.0 mmol) were then added and the reaction mixture was stirred at room temperature for 24 h. The volatiles were concentrated under reduced pressure and the resulting crude product was dissolved in 100 mL of CH_2Cl_2. The organic phase was washed sequentially with aqueous saturated solution of citric acid (50 mL), aqueous 10% $NaHCO_3$ (50 mL), and brine (50 mL), and then dried over anhydrous

Na_2SO_4 and concentrated under reduced pressure. The resulting amorphous solid was used in the Boc deprotection step without further purification.

Microwave-assisted Ugi-4CR-based: The amine (1.0 mmol) and the aldehyde (1.0 mmol) were dissolved in MeOH (5 mL) and added to a 10 mL glass tube. NEt_3 (1.0 mmol) was added when α-amino acid methyl ester hydrochlorides were employed. The suspension was treated with the carboxylic acid (1.0 mmol) and the isocyanide (1.0 mmol) and the glass tube was sealed and introduced in the microwave reactor. The flask was irradiated for 30 min (150 W) under high-speed magnetic stirring, while the temperature was raised up to 70 °C. The reaction course was monitored by TLC, and additional cycles of 30 min were applied in cases of poor consumption of the starting material. The volatiles were concentrated under reduced pressure and the resulting crude product was dissolved in 100 mL of CH_2Cl_2. The organic phase was washed sequentially with aqueous saturated solution of citric acid (50 mL), aqueous 10% $NaHCO_3$ (2×50 mL), and brine (50 mL), and then dried over anhydrous Na_2SO_4 and concentrated under reduced pressure. The resulting amorphous solid was used in the Boc deprotection step without further purification.

General Boc deprotection procedure: The crude product resultant form the Ugi-4CR was dissolved in 3 mL of CH_2Cl_2 and treated with 1 mL of trifluoroacetic acid at 0 °C. The reaction mixture was allowed to reach room temperature, stirred for 4 h and then concentrated to dryness (TFA was removed completely by repetitive addition and evaporation of further CH_2Cl_2). The crude product was re-dissolved in 10 mL of CH_2Cl_2, treated with solid K_2CO_3 until basic pH and the solution was filtered and evaporated under reduced pressure.

Peptide-peptoid hybrid 1: HCl·Gly-OMe (125 mg, 1 mmol), triethylamine (140 µL, 1 mmol) paraformaldehyde (30 mg, 1 mmol), Boc-L-Pro-OH (215 mg, 1 mmol) and cyclohexylisocyanide (125 µL, 1 mmol) were reacted in MeOH (5 mL) according to the general Ugi-4CR-based procedure. The resulting Boc protected compound was subjected to

the general deprotection procedure. Flash column chromatography purification (MeOH/EtOAc 4:1) afforded peptide-peptoid hybrid **1** (254 mg, 78%) as a colorless oil. R_f = 0.25 (*n*-hexane/EtOAc 1:1). $[\alpha]_D^{20}$ -15.1 (*c* 0.62, MeOH, 25°C). A mixture of conformers in a 6:4 ratio was observed by NMR. ^{1}H NMR (400 MHz, $CDCl_3$): δ = 1.09-1.40 (m, 6H); 1.55-1.95 (m, 6H); 1.99-2.17 (m, 3H); 2.41 (m, 1H); 3.37-3.50 (m, 2H); 3.67-3.80 (m, 1H); 3.76, 3.80 (2×s, 3H); 4.10 (d, 1H, *J* = 17.2 Hz); 4.15 (m, 1H); 4.31 (d, 1H, *J* = 17.2 Hz); 4.96 (m, 1H); 6.95, 7.48 (2×d, 1H, *J* = 8.0 Hz). ^{13}C NMR (100 MHz, $CDCl_3$): δ = 24.8, 24.9, 25.3, 29.0, 32.5, 46.4, 49.4, 51.7, 52.7, 53.4, 57.9, 165.9, 169.6, 170.1. HRMS (ESI-FT-ICR) *m/z*: 326.2072 $[M+H]^+$; calcd. for $C_{16}H_{28}N_3O_4$: 326.2069.

Peptide-peptoid hybrid 2: HCl·Val-OMe (168 mg, 1 mmol), triethylamine (140 µL, 1 mmol) paraformaldehyde (30 mg, 1 mmol), Boc-L-Pro-OH (215 mg, 1 mmol) and cyclohexylisocyanide (125 µL, 1 mmol) were reacted in MeOH (5 mL) according to the microwave-assisted Ugi-4CR-based procedure, using two cycles of 30 min. The resulting Boc protected compound was subjected to the general deprotection procedure. Flash column chromatography purification (MeOH/EtOAc 4:1) afforded peptide-peptoid hybrid **2** (297.7 mg, 81%) as a colorless oil. R_f = 0.45 (*n*-hexane/EtOAc 1:1). $[\alpha]_D^{20}$ -56.1 (*c* 0.56, MeOH, 25°C). A mixture of conformers in a 7:3 ratio was observed by NMR. ^{1}H NMR (400 MHz, $CDCl_3$): δ = 0.87 (d, 3H, *J* = 6.6 Hz); 0.98 (d, 3H, *J* = 6.6 Hz); 1.06-1.39 (m, 5H); 1.54-1.91 (m, 5H); 1.94-2.54 (br. m, 5H); 3.16-3.34 (m, 1H); 3.38-3.53 (m, 2H); 3.72, 3.74 (2×s, 3H); 3.62-3.76 (m, 1H); 3.95, 4.15 (2×d, 1H, *J* = 16 Hz); 4.13, 4.25 (2×d, 1H, *J* = 18 Hz); 3.81, 4.46 (2×d, 1H, *J* = 10.4/9.7 Hz); 4.78, 4.85(2×m, 1H); 6.59, 7.11 (2×d, 1H, *J* = 7.8 Hz). ^{13}C NMR (100 MHz, $CDCl_3$): δ = 15.8, 20.0, 21.7, 24.6, 25.5, 29.5, 30.9, 32.8, 32.9, 44.5, 48.2, 51.1, 58.8, 67.6, 163.1, 167.5, 168.2. HRMS (ESI-FT-ICR) *m/z*: 368.2543 $[M+H]^+$; calcd. for $C_{19}H_{34}N_3O_4$: 368.2538.

Peptide-peptoid hybrid 3: HCl·Leu-OMe (182 mg, 1 mmol), triethylamine (140 µL, 1 mmol) paraformaldehyde (30 mg, 1 mmol), Boc-L-Pro-OH (215 mg, 1 mmol) and cyclohexylisocyanide (125 µL, 1 mmol) were reacted in MeOH (5 mL) according to the microwave-assisted Ugi-4CR-based procedure, using two cycles of 30 min. The resulting Boc protected compound was subjected to the general deprotection procedure. Flash column chromatography purification (MeOH/EtOAc 4:1) afforded peptide-peptoid hybrid **3** (324 mg, 85%) as a colorless oil. R_f = 0.50 (*n*-hexane/EtOAc 1:1). $[\alpha]_D^{20}$ -42.7 (*c* 0.66, MeOH, 25°C). A mixture of conformers in a 7:3 ratio was observed by NMR. ^{1}H NMR (400 MHz, $CDCl_3$): δ = 0.84-1.00 (m, 6H); 1.07-1.39 (m, 5H); 1.54-1.91(m, 7H); 1.98-2.23 (m, 2H); 2.44 (m, 1H); 3.05 (br. s, 1H); 3.40-3.50 (m, 2H); 3.64-3.71 (m, 2H); 3.74 (s, 3H); 4.04 (d, 1H, *J* = 18.2 Hz); 4.19 (d, 1H, *J* = 18.2 Hz); 4.32 (2×d, 1H, *J* = 8.8/5.1 Hz); 4.66 (t, 1H, *J* = 7.1 Hz); 4.79 (t, 1H, *J* = 7.1 Hz); 6.59, 7.56 (2×d, 1H, *J* = 7.7 Hz). ^{13}C NMR (100 MHz, $CDCl_3$): δ = 22.1, 22.4, 24.6, 24.9, 25.0, 25.3, 29.1, 32.3, 37.6, 38.4, 46.2, 49.2, 49.4, 52.7, 58.1, 58.3, 166.5, 170.4, 172.2. HRMS (ESI-FT-ICR) *m/z*: 382.2700 $[M+H]^+$; calcd. for $C_{20}H_{36}N_3O_4$: 382.2698.

Peptide-peptoid hybrid 4: HCl·Ile-OMe (182 mg, 1 mmol), triethylamine (140 µL, 1 mmol) paraformaldehyde (30 mg, 1 mmol), Boc-L-Pro-OH (215 mg, 1 mmol) and cyclohexylisocyanide (125 µL, 1 mmol) were reacted in MeOH (5 mL) according to the microwave-assisted Ugi-4CR-based procedure, using two cycles of 30 min. The resulting Boc protected compound was subjected to the general deprotection procedure. Flash column chromatography purification (MeOH/EtOAc 4:1) afforded peptide-peptoid hybrid **4** (294 mg, 77%) as a colorless oil. R_f = 0.50 (*n*-hexane/EtOAc 1:1). $[\alpha]_D^{20}$ -59.1 (*c* 0.65, MeOH, 25°C). A mixture of conformers in a 1:1 ratio was observed by NMR. ^{1}H NMR (400 MHz, $CDCl_3$): δ = 0.86 (t, 3H, *J* = 7.35 Hz); 0.94 (d, 3H, *J* = 6.5 Hz); 1.01-1.44 (m, 6H); 1.49-2.26 (m, 10H); 2.40, 2.49 (2×m, 1H); 3.46 (m, 2H); 3.63-3.71 (m, 1H); 3.73 (s, 3H); 4.02, 4.16 (2×d, 1H, *J* = 16.0 Hz); 4.14, 4.26 (2×d, 1H, *J* = 18.2 Hz); 3.88, 4.66 (2×d, 1H, *J* = 10.0 Hz); 4.81, 4.90

(2×t, 1H, *J* = 8.0 Hz); 6.46, 6.85 (2×d, 1H, *J* = 8.0 Hz). ^{13}C NMR (100 MHz, $CDCl_3$): δ = 11.4, 15.7, 24.8, 25.2, 25.3, 25.6, 29.5, 32.4, 34.1, 46.3, 46.6, 47.00, 47.8, 48.9, 52.6, 58.4, 63.1, 166.6, 169.4, 170.9. HRMS (ESI-FT-ICR) *m/z*: 382.2700 $[M+H]^+$; calcd. for $C_{20}H_{36}N_3O_4$: 382.2695.

Peptide-peptoid hybrid 5: HCl·Phe-OMe (216 mg, 1 mmol), triethylamine (140 µL, 1 mmol) paraformaldehyde (30 mg, 1 mmol), Boc-L-Pro-OH (215 mg, 1 mmol) and cyclohexylisocyanide (125 µL, 1 mmol) were reacted in MeOH (5 mL) according to the microwave-assisted Ugi-4CR-based procedure, using two cycles of 30 min. The resulting Boc protected *pseudo*-peptide was subjected to the general deprotection procedure. Flash column chromatography purification (MeOH/EtOAc 4:1) afforded peptide-peptoid hybrid **5** (345 mg, 83%) as a light yellow oil. R_f = 0.35 (*n*-hexane/EtOAc 1:1). $[\alpha]_D^{20}$ -87.6 (*c* 0.47, MeOH, 25°C). A mixture of conformers in a 7:3 ratio was observed by NMR. ^{1}H NMR (400 MHz, $CDCl_3$): δ = 1.06-1.43 (m, 5H); 1.52-1.99 (m, 5H); 2.08 (m, 2H); 2.30 (m, 1H); 3.22-3.54 (m, 4H); 3.66 (m, 1H); 3.77 (s, 3H); 4.20 (m, 1H); 4.25 (dd, 1H, *J* = 10.0/5.9 Hz); 4.55 (dd, 1H, *J* = 7.2 Hz); 7.12-7.14 (m, 1H); 7.18-7.38 (m, 4H); 7.71 (d, 1H, *J* = 7.8 Hz). ^{13}C NMR (100 MHz, $CDCl_3$): δ = 24.7, 24.9, 25.0, 25.3, 29.1, 32.4, 34.4, 46.1, 49.2, 52.6, 53.0, 57.9, 63.8, 127.5, 128.4, 129.0, 129.2, 129.9, 136.2, 165.4, 169.5, 170.4. HRMS (ESI-FT-ICR) *m/z*: 416.2541 $[M+H]^+$; calcd. for $C_{23}H_{34}N_3O_4$: 416.2535.

Peptide-peptoid hybrid 6: HCl·*t*BuGly-OMe (182 mg, 1 mmol), triethylamine (140 µL, 1 mmol) paraformaldehyde (30 mg, 1 mmol), Boc-L-Pro-OH (215 mg, 1 mmol) and cyclohexylisocyanide (125 µL, 1 mmol) were reacted in MeOH (5 mL) according to the microwave-assisted Ugi-4CR-based procedure, using three cycles of 30 min. The resulting Boc protected compound was subjected to the general deprotection procedure. Flash column chromatography purification (MeOH/EtOAc 4:1) afforded peptide-peptoid hybrid **6** (233 mg, 61%) as a colorless oil. R_f = 0.55 (*n*-hexane/EtOAc 1:1). $[\alpha]_D^{20}$ -5.9 (*c* 0.43, MeOH, 25°C). A

mixture of conformers in a 1:1 ratio was observed by NMR. ^{1}H NMR (400 MHz, $CDCl_3$): δ = 1.05, 1.09 (2×s, 9H); 1.00-1.43 (m, 3H); 1.55-2.02 (m, 13H); 2.19 (m, 1H); 2.50 (m, 1H); 2.81 (m, 1H); 3.13 (m, 1H); 3.55-3.65 (m, 1H); 3.73, 3.80 (2×s, 3H); 3.67-3.77 (m, 1H); 4.12 (dd, 1H, *J* = 7.7/3.1 Hz); 4.18, 4.29 (2×d, 1H, *J* = 18.4 Hz); 5.12 (s, 1H). ^{13}C NMR (100 MHz, $CDCl_3$): δ = 23.2, 25.1, 25.4, 25.6, 27.8, 28.1, 28.6, 30.8, 32.8, 36.4, 45.6, 47.8, 50.7, 51.8, 59.2, 62.0, 164.3, 169.6, 170.0 HRMS (ESI-FT-ICR) *m/z*: 382.2700 $[M+H]^+$; calcd. for $C_{20}H_{36}N_3O_4$: 382.2695.

Peptide-peptoid hybrid 7: (*S*)-α-Methylbenzylamine (128 µL, 1 mmol), paraformaldehyde (30 mg, 1 mmol), Boc-L-Pro-OH (215 mg, 1 mmol) and cyclohexylisocyanide (125 µL, 1 mmol) were reacted in MeOH (5 mL) according to the general Ugi-4CR-based procedure. The resulting Boc protected compound was subjected to the general deprotection procedure. Flash column chromatography purification (MeOH/EtOAc 4:1) afforded peptide-peptoid hybrid **7** (325 mg, 91%) as a colorless oil. R_f = 0.55 (*n*-hexane/EtOAc 1:1). $[\alpha]_D^{20}$ -62.8 (*c* 0.64, MeOH, 25°C). A mixture of conformers in a 6:4 ratio was observed by NMR. ^{1}H NMR (400 MHz, $CDCl_3$): δ = 1.01-1.36 (m, 5H); 1.49, 169 (2×d, 3H, *J* = 7.2 Hz); 1.47-1.84 (m, 4H); 2.17 (m, 2H); 3.40, 2.54 (2×m, 1H); 2.85 (br. m, 1H); 3.45 (m, 2H); 3.61 (m, 1H); 3.71, 3.89 (2×d, 1H, *J* = 18.0 Hz); 3.51, 3.93 (2×d, 1H, *J* = 16.0 Hz); 4.70, 5.10 (2×m, 1H); 5.87, 6.35 (2×q, 1H, *J* = 7.25 Hz); 7.22-7.40 (m, 5H); 7.72 (br. s, 1H). ^{13}C NMR (100 MHz, $CDCl_3$): δ = 17.4; 24.9, 25.3, 29.8, 32.2, 32.5, 46.1, 46.6, 48.7, 49.2, 55.6, 58.2, 60.4, 127.1, 127.4, 128.6, 128.8, 129.1, 137.7, 162.7, 166.5. HRMS (ESI-FT-ICR) *m/z*: 358.2489 $[M+H]^+$; calcd. for $C_{21}H_{32}N_3O_2$: 358.2483.

Peptide-peptoid hybrid 8: Benzylamine (110 µL, 1 mmol), paraformaldehyde (30 mg, 1 mmol), Boc-L-Pro-OH (215 mg, 1 mmol) and cyclohexylisocyanide (125 µL, 1 mmol) were reacted in MeOH (5 mL) according to the general Ugi-4CR-based procedure. The resulting Boc protected compound was subjected to the general deprotection procedure. Flash column

chromatography purification (MeOH/EtOAc 4:1) afforded peptide-peptoid hybrid **8** (639 mg, 93%) as a pale green oil. R_f = 0.35 (*n*-hexane/EtOAc 1:1). $[\alpha]_D^{20}$ -21.1 (*c* 0.41, MeOH, 25°C). A mixture of conformers in a 7:3 ratio was observed by NMR. ^{1}H NMR (400 MHz, $CDCl_3$): δ = 1.05-1.37 (m, 5H); 1.52-1.85 (m, 4H); 1.96-2.10 (m, 3H); 2.23, 2.38 (2×m, 1H); 2.83 (br. s, 1H); 3.39-3.55 (m, 2H); 3.69 (m, 1H); 3.97 (m, 2H); 4.66 (m, 2H); 4.79, 4.90 (2×m, 1H); 6.76 (d, 1H, *J* = 8.0 Hz); 7.18-7.40 (m, 5H). ^{13}C NMR (100 MHz, $CDCl_3$): δ = 24.8, 25.0, 25.4, 29.5, 32.5, 45.9, 48.8, 49.3, 50.8, 52.2, 58.3, 127.3, 128.3, 128.5, 128.9, 129.3, 134.2, 166.4, 170.0. HRMS (ESI-FT-ICR) *m/z*: 344.2331 $[M+H]^+$; calcd. for $C_{20}H_{30}N_3O_2$: 344.2328

Peptide-peptoid hybrid 9: (*S*)-α-Methylbenzylamine (128 µL, 1 mmol), acetone (74 µL, 1 mmol), Boc-L-Pro-OH (215 mg, 1 mmol) and cyclohexylisocyanide (125 µL, 1 mmol) were reacted in MeOH (5 mL) according to the general Ugi-4CR-based procedure. The resulting Boc protected compound was subjected to the general deprotection procedure. Flash column chromatography purification (MeOH/EtOAc 4:1) afforded peptide-peptoid hybrid **9** (309 mg, 77%) as a colorless oil. R_f = 0.35 (*n*-hexane/EtOAc 1:1). $[\alpha]_D^{20}$ -1.9 (*c* 0.38, MeOH, 25°C). ^{1}H NMR (600 MHz, $CDCl_3$): δ = 1.17-1.23 (m, 4H, CH_2); 1.27-1.37 (m, 2H, CH_2); 1.41-1.46 (m, 2H, CH_2); 1.48 (s, 3H, CH_3); 1.55 (m, 3H, CH_3); 1.66-1.92 (m, 4H, CH_2); 1.87 (d, 3H, *J* = 7.0 Hz, CH_3); 2.13 (m, 1H, CH_2); 2.33 (m, 1H, CH_2); 3.24 (m, 2H, CH_2); 3.37 (m, 1H, CH_2); 3.60 (m, 1H, C*H*); 4.30 (m, 1H, C*H*); 5.11 (m, 1H, C*H*); 5.74 (d, 1H, *J* = 7.3 Hz, N*H*); 7.24 (t, 1H, *J* = 7.5 Hz, C*H*); 7.36 (t, 2H, *J* = 7.6 Hz, C*H*); 7.57 (d, 2H, *J* = 7.7 Hz, C*H*). ^{13}C NMR (150 MHz, $CDCl_3$): δ = 19.2 (*C*H_3); 24.3, 24.7, 24.9, 25.0, 25.5 (*C*H_2); 27.8, 28.4 (*C*H_3); 28.9, 32.7, 46.3 (*C*H_2); 48.9, 51.8, 59.7 (*C*H); 64.9 (*C*); 127.3, 128.0, 129.2 (*C*H); 140.8 (*C*); 170.8, 173.4 (*C*=O). HRMS (ESI-FT-ICR) *m/z*: 386.2800 $[M+H]^+$; calcd. for $C_{23}H_{36}N_3O_2$: 386.2802.

Peptide-peptoid hybrid 10: Benzylamine (110 µL, 1 mmol), acetone (74 µL, 1 mmol), Boc-L-Pro-OH (215 mg, 1 mmol) and cyclohexylisocyanide (125 µL, 1 mmol) were reacted in MeOH (5 mL) according to the general Ugi-4CR-based procedure. The resulting Boc

protected compound was subjected to the general deprotection procedure. Flash column chromatography purification (MeOH/EtOAc 4:1) afforded peptide-peptoid hybrid **10** (229 mg, 73%) as a colorless oil. R_f = 0.35 (*n*-hexane/EtOAc 1:1). $[\alpha]_D^{20}$ -20.6 (*c* 0.41, MeOH, 25°C). ^{1}H NMR (400 MHz, $CDCl_3$): δ = 1.06-1.39 (m, 5H); 1.46 (s, 3H); 1.50 (s, 3H); 1.55-1.75 (m, 3H); 1.78-2.06 (m, 6H); 3.03 (br. m, 1H); 3.40 (m, 2H); 3.68 (m, 1H); 4.69 (m, 1H); 4.76 (d, 2H, *J* = 6.91 Hz); 5.98 (d, 1H, *J* = 8.0 Hz); 7.22-7.44 (m, 5H). ^{13}C NMR (100 MHz, $CDCl_3$): δ = 24.1, 24.5, 24.9, 25.4, 29.7, 32.6, 32.7, 46.0, 47.9, 48.8, 58.9, 64.1, 126.4, 128.0, 129.2, 136.9, 169.9, 173.0. HRMS (ESI-FT-ICR) *m/z*: 372.2651 $[M+H]^+$; calcd. for $C_{22}H_{33}N_3O_2$: 372.2654.

Peptide-peptoid hybrid 11: (*S*)-α-Methylbenzylamine (128 µL, 1 mmol), paraformaldehyde (30 mg, 1 mmol), Boc-L-Pro-OH (215 mg, 1 mmol) and *t*-butylisocyanide (125 µL, 1 mmol) were reacted in MeOH (5 mL) according to the general Ugi-4CR-based procedure. The resulting Boc protected compound was subjected to the general deprotection procedure. Flash column chromatography purification (MeOH/EtOAc 4:1) afforded peptide-peptoid hybrid **11** (298 mg, 88%) as a light yellow oil. R_f = 0.55 (*n*-hexane/EtOAc 1:1). $[\alpha]_D^{20}$ -78.9 (*c* 0.65, MeOH, 25°C). A mixture of conformers in a 8:2 ratio was observed by NMR. ^{1}H NMR (400 MHz, $CDCl_3$): δ = 1.23, (2×s, 6H); 1.49 (2×s, 3H); 1.46, 1.68 (2×d, 3H, *J* = 6.88 Hz); 1.87-2.25 (m, 3H); 2.42, 2.58 (2×m, 1H); 3.32-3.55 (m, 1H); 3.61, 3.88 (2×d, 1H, *J* = 18.0 Hz); 3.45, 3.95 (2×d, 1H, *J* = 16.0 Hz); 4.98, 5.11 (2×m, 1H); 5.78 (m, 1H); 7.24-7.39 (m, 5H); 7.80 (br. s, 1H). ^{13}C NMR (100 MHz, $CDCl_3$): δ = 17.4, 24.9, 28.4, 28.5, 29.9, 46.9, 47.0, 51.3, 53.6, 55.5, 58.2, 125.8, 127.0, 128.6, 128.8, 129.2, 137.9, 167.2, 170.2. HRMS (ESI-FT-ICR) *m/z*: 332.2330 $[M+Na]^+$; calcd. for $C_{19}H_{30}N_3O_2$: 332.2327.

Peptide-peptoid hybrid 12: (*S*)-α-Methylbenzylamine (128 µL, 1 mmol), paraformaldehyde (30 mg, 1 mmol), Boc-L-Pro-OH (215 mg, 1 mmol) and methyl isocyanoacetate (91 µL, 1 mmol) were reacted in MeOH (5 mL) according to the general Ugi-4CR-based procedure.

The resulting Boc protected compound was subjected to the general deprotection procedure. Flash column chromatography purification (MeOH/EtOAc 4:1) afforded peptide-peptoid hybrid **12** (590.6 mg, 82%) as a light yellow oil. R_f = 0.45 (*n*-hexane/EtOAc 1:1). $[\alpha]_D^{20}$ -18.9 (*c* 0.65, MeOH, 25°C). A mixture of conformers in a 7:3 ratio was observed by NMR. ^{1}H NMR (400 MHz, $CDCl_3$): δ =1.55, 1.71 (2×d, 3H, *J* = 6.8 Hz); 2.17 (m, 3H); 2.51 (m, 4H); 3.37-3.55 (m, 2H); 3.65, 3.70 (2×s, 3H); 3.62, 3.81 (2×d, 1H, *J* = 18.0 Hz); 3.55, 4.02 (2×d, 1H, *J* = 16.2 Hz); 4.69, 4.98 (2×m, 1H); 5.08, 5.95 (2×m, 1H); 7.22-7.36 (m, 5H); 8.35 (m, 1H). ^{13}C NMR (100 MHz, $CDCl_3$): δ = 17.4, 24.6, 29.1, 40.8, 45.6, 46.3, 52.2, 52.3, 55.6, 58.8, 127.0, 127.1, 128.6, 128.9, 129.0, 137.6, 168.8, 171.1. HRMS (ESI-FT-ICR) *m/z*: 348.1917 $[M+H]^+$; calcd. for $C_{18}H_{25}N_3O_4$: 348.1915.

Peptide-peptoid hybrid 13: (*S*)-α-Methylbenzylamine (128 µL, 1 mmol), acetone (74 µL, 1 mmol), Boc-D-Pro-OH (215 mg, 1 mmol) and cyclohexylisocyanide (125 µL, 1 mmol) were reacted in MeOH (5 mL) according to the general Ugi-4CR-based procedure. The resulting Boc protected compound was subjected to the general deprotection procedure. Flash column chromatography purification (MeOH/EtOAc 4:1) afforded peptide-peptoid hybrid **13** (317 mg, 77%) as a colorless oil. R_f = 0.36 (*n*-hexane/EtOAc 1:1). $[\alpha]_D^{20}$ +15.6 (*c* 0.44, MeOH, 25°C). ^{1}H NMR (400 MHz, $CDCl_3$): δ = 1.07-1.41 (m, 8H); 1.54 (s, 3H); 1.57 (s, 3H); 1.61 (m, 2H); 1.67-1.83 (m 2H); 1.87 (d, 3H, *J* = 7.2 Hz); 1.89-2.00 (m, 3H); 2.71 (m, 1H); 3.09 (m, 2H); 3.70 (m, 2H); 5.17 (m, 1H); 5.58 (d, 1H, *J* = 6.3 Hz); 7.28-7.27-7.41 (m, 3H); 7.49 (d, 2H, *J* = 8.0 Hz). ^{13}C NMR (100 MHz, $CDCl_3$): δ = 20.8, 25.2, 24.9, 25.6, 26.5, 28.5, 31.4, 32.9, 47.5, 48.4, 60.0, 64.4, 126.0, 127.2, 128.8, 142.2, 170.4, 173.9. HRMS (ESI-FT-ICR) *m/z*: 386.2807 $[M+H]^+$; calcd. for $C_{23}H_{36}N_3O_2$: 386.2802.

General procedure for the 1,4-addition of aldehydes to nitroolefins (Michael reaction): The nitroolefin (0.25 mmol, 1.0 equivalent) and the aldehyde (0.75 mmol, 3.0 equivalents) were added to a solution of the *pseudo*-peptide (0.025 mmol, 0.01 equivalent.) in the solvent

of choice (1 mL). The reaction mixture was stirred for 24 h and then concentrated under reduced pressure. The resulting crude product was purified by flash column chromatography on silica gel using *n*-hexane/EtOAc as eluent. The enantiomeric excess was determined by chiral-phase HPLC analysis through comparison with the authentic racemic material. Assignment of the stereoisomers was performed by comparison with literature data.

(2*R*,3*S*)-2-Ethyl-4-nitro-3-phenylbutanal (14): Prepared by reaction of *n*-butanal with *trans*-β-nitrostyrene according to the general 1,4-addition procedure. The compound was purified by flash column chromatography *n*-hexane/EtOAc 9:1 *v/v*). The spectroscopic data are in agreement with the published data.[16b] The enantiomeric excess was determined by chiral-phase HPLC (Chiralpak AD-H, *n*-hexane/*i*-PrOH 99:1, 25°C) at 0.75 ml/min, UV detection at 210 nm: t_R: (*syn*, major) = 24.6 min, (*syn*, minor) = 29.3 min.

(2*R*,3*S*)-2-Isopropyl-4-nitro-3-phenylbutanal (15): Prepared from isovaleraldehyde and *trans*-β-nitrostyrene according to the general 1,4-addition procedure. The compound was purified by flash column chromatography *n*-hexane/EtOAc 9:1 *v/v*). The spectroscopic data are in agreement with the published data.[16b] The enantiomeric excess was determined by HPLC (Chiralpak AD-H, *n*-hexane/*i*-PrOH 97:3, 25°C) at 0.4ml/min, UV detection at 210 nm: t_R: (*syn*, major) = 24.5 min, (*syn*, minor) = 28.9 min.

(2*R*,3*S*)-2-Ethyl-4-nitro-3-(4-methoxyphenyl)butanal (16): Prepared from *n*-butanal and 1-methoxy-4-(2-nitrovinyl)benzene according to the general procedure. The spectroscopic data are in agreement with the published data.[21] The enantiomeric excess was determined by chiral-phase HPLC (Chiralpak AD-H, *n*-hexane/*i*-PrOH 95:5, 25°C) at 0.8ml/min, UV detection at 210 nm: t_R: (*syn*, major) = 16.9 min, (*syn*, minor) = 20.8 min.

(2*R*,3*S*)-3-(4-Fluorophenyl)-2-ethyl-4-nitrobutanal (17): Prepared from *n*-butanal and *trans*-4-fluoro-β-nitrostyrene according to the general 1,4-addition procedure. The compound was purified by flash column chromatography *n*-hexane/EtOAc 9:1 *v/v*). The spectroscopic

data are in agreement with the published data.[8a] The enantiomeric excess was determined by HPLC (Chiralpak AD-H, *n*-hexane/*i*-PrOH 95:5, 25°C) at 0.8ml/min, UV detection at 210 nm: t_R: (*syn*, major) = 15.4 min, (*syn*, minor) = 19.3 min.

(*2R,3S*)-3-(4-Chlorophenyl)-2-ethyl-4-nitrobutanal (18): Prepared from *n*-butanal and *trans*-4-chloro-β-nitrostyrene according to the general 1,4-addition procedure. The compound was purified by flash column chromatography *n*-hexane/EtOAc 9:1 *v/v*). The spectroscopic data are in agreement with the published data.[8a] The enantiomeric excess was determined by HPLC (Chiralpak AD-H, *n*-hexane/*i*-PrOH 95:5, 25°C) at 0.8ml/min, UV detection at 210 nm: t_R: (*syn*, major) = 15.4 min, (*syn*, minor) = 19.3 min.

(*2R,3S*)-3-(4-Bromophenyl)-2-ethyl-4-nitrobutanal (19): Prepared from *n*-butanal and *trans*-4-bromo-β-nitrostyrene according to the general 1,4-addition procedure. The compound was purified by flash column chromatography *n*-hexane/EtOAc 9:1 *v/v*). The spectroscopic data are in agreement with the published data.[8a] The enantiomeric excess was determined by HPLC (Chiralpak AD-H, *n*-hexane/*i*-PrOH 95:5, 25°C) at 0.8ml/min, UV detection at 210 nm: t_R: (*syn*, major) = 15.4 min, (*syn*, minor) = 19.3 min.

(*2R,3S*)-3-(2-Bromophenyl)-2-ethyl-4-nitrobutanal (20): Prepared from *n*-butanal and *trans*-2-bromo-β-nitrostyrene according to the general 1,4-addition procedure. The compound was purified by flash column chromatography *n*-hexane/EtOAc 9:1 *v/v*). The spectroscopic data are in agreement with the published data.[8a] The enantiomeric excess was determined by HPLC (Chiralpak AD-H, *n*-hexane/*i*-PrOH 97:3, 25°C) at 0.5ml/min, UV detection at 210 nm: t_R: (*syn*, major) = 20.8 min, (*syn*, minor) = 23.1 min.

(*2R,3S*)-2-Ethyl-4-nitro-3-(3-nitrophenyl)butanal (21): Prepared from *n*-butanal and 1-nitro-3-(2-nitrovinyl)benzene according to the general 1,4-addition procedure. The compound was purified by flash column chromatography *n*-hexane/EtOAc 9:1 *v/v*). The spectroscopic data are in agreement with the published data.[22] The enantiomeric excess was determined by

HPLC (Chiralpak AD-H, *n*-hexane/*i*-PrOH 95:5, 25°C) at 0.8ml/min, UV detection at 210 nm: t_R: (*syn*, major) = 36.0 min, (*syn*, minor) = 39.1 min.

(*2R,3S*)-2-Ethyl-4-nitro-3-(2-furyl)butanal (22): Prepared from *n*-butanal and *trans*-2-(2-nitrovinyl)furan according to the general 1,4-addition procedure. The compound was purified by flash column chromatography *n*-hexane/EtOAc 9:1 *v/v*). The spectroscopic data are in agreement with the published data.[22] The enantiomeric excess was determined by HPLC (Chiralpak AD-H, *n*-hexane/*i*-PrOH 97:3, 25°C) at 0.5ml/min, UV detection at 210 nm: t_R: (*syn*, major) = 22.1 min, (*syn*, minor) = 23.9 min

Computational Methods

The conformational searches were done in gas phase using the Monte Carlo (MCMM) method. The energy minimization was carried out using the Polak-Ribiere Conjugate Gradient (PRCG),[23] and the MMFF force field,[24] using dielectric constant-dependent electrostatics (e=1) and normal cut-off points to model the non-bonded interactions, as implemented in MacroModel (Version 9.9).[25] All heavy atoms and hydrogens at heteroatoms were included in the test for redundant conformers, using the default cutoff (maximum atom deviation) of 0.5 Å. All rotatable single bonds were included in the conformational search, even the N-C=O amide single bond. The energy window for saving new structures was 5 kcal/mol relative to the current global minimum, using a maximum number of steps of 30000 and 1000 steps per rotable bond. Each search was continued until the global energy minima were found at least 10-20 times, thus giving confidence that all the relevant conformers had been found.

The cluster analyses were performed using a python script "Clustering of Conformers" interfaced to the Maestro (Version 9.3) program,[26] and available in Schrödinger script-center website.[27] Several works have shown the cluster analysis in the precise description of organic molecules in solution.[28] To generate the RMS matrix, all heavy atoms and hydrogens at heteroatoms were included. The *average* method was used to calculate the best number of

cluster in all cases. The low-energy structures of each cluster were selected and submitted to a full geometry optimization using Quantum Mechanics. All conformers were clustered and graphically represented in supporting information B.

The representative (low energy) structures of each cluster were fully optimized using the Truhlar M06-2X[29] density functional in conjunction with the 6-31G(d) basis set through the Gaussian09 program.[30] The SMD model[31] was used for inclusion of the solvent effect for all optimizations. All Cartesian coordinates are supplied in the SI. Frequency calculations at 295.15 K (1 atm) ensured that the stationary points represent either minima (no imaginary frequency) or transition states (single imaginary frequency) on the potential-energy surface, furnishing also the zero-point vibrational energies, the thermal and entropic correction from which the Gibbs free energies were determined. The corresponding eigenvectors were inspected to confirm the expected isomerization transition state. The electronic energies were further refined using 6-31+g(d,p) basis set. The natural bond orbital (NBO) analysis was calculated at M06-2X/6-31+G(d,p) level using NBO 5.0 program as implemented in Gaussian 09.

Acknowledgements

A. F. de la Torre and M. W. Paixão thanks CNPq for a PhD and Research fellowships, respectively. D. G. Rivera is grateful to CAPES for a Visiting Professor Program. We are in debit to Prof. Claudio Tormena for computational facilities support. We also gratefully acknowledge financial support from CNPq (INCT-Catálise), CAPES (CAPES-MES/Cuba Program) and FAPESP (2009/07281-0 and 2013/02311-3).

Supporting Information. ^{1}H and ^{13}C NMR spectra of peptide-peptoid hybrid catalysts and chiral-phase HPLC analysis of Michael adducts. Complete computational data and geometries of re-optimized low-energy conformers. This material is available free of charge via the Internet at http://pubs.acs.org.

References

[1] a) Notz, W.; Tanaka, F.; Barbas, C. F. *Acc. Chem. Res.* **2004**, *37*, 580-591; b) Grondal, C.; Jeanty, M.; Enders, D. *Nature Chem.* **2010**, *2*, 167-178; c) Enders, D.; Grondal, C.; Hüttl, M. R. M. *Angew. Chem. Int. Ed.* **2007**, *46*, 1570-1581; d) Beeson, T. D.; Mastracchio, A.; Hong, J.-B.; Ashton, K.; MacMillan, D. W. C. *Science* **2007**, *316,* 582-585; e) Mukherjee, S.; Yang, J. W.; Hoffmann, S.; List, B. *Chem. Rev.* **2007**, *107*, 5471-5569; f) Doyle, A. G.; Jacobsen, E. N. *Chem. Rev*. **2007**, *107*, 5713-5743; g) Melchiorre, P.; Marigo, M.; Carlone, A.; Bartoli. G. *Angew. Chem. Int. Ed*. **2008**, *47*, 6138-6171; h) Bertelsen, S.; Jørgensen. K. A. *Chem. Soc. Rev*. **2009**, *38*, 2178-2189; i) Tan, B.; Candeias, N. R.; Barbas, C. F. *Nature Chem.* **2011**, *3*, 473-477; j) Jensen, K. L.; Dickmeiss, G.; Jiang, H.; Albrecht, L.; Jørgensen, K. A. *Acc. Chem. Res*. **2012**, *45*, 248-264; k) Hernandez, J. G.; Juaristi, E. *Chem. Commun.* **2012**, *48*, 5396-5409; l) Melchiorre. P. *Angew. Chem. Int. Ed*. **2012**, *51*, 9748-9770.

[2] For selected reviews, see: a) Wennemers, H. *Chem. Commun.* **2011**, *47*, 12036-12041; b) Freund, M.; Tsogoeva S. B. In Catalytic Methods in Asymmetric Synthesis: Advanced Materials, Techniques, and Applications; Gruttadauria, M.; Giacalone F., Eds.; Wiley: Hoboken, **2011**, pp. 529-578; c) Davie, E. A. C.; Mennen, S. M.; Xu, Y.; Miller, S. J. *Chem. Rev.* **2007**, *107*, 5759-5812, d) Miller, S. J. *Acc. Chem. Res*. **2004**, *37*, 601-610.

[3] For selected reviews and recent reports on combinatorial methods for catalysts discovery and development, see: a) Lichtor, P. A.; Miller, S. J. *Nature Chem.* **2012**, *4*, 990-995; b) Lichtor, P. A.; Miller, S. J. *ACS Comb. Sci.* **2011**, *13*, 321-326; c) Revell, J. D.; Wennemers, H. *Top. Curr. Chem.* **2007**, *277*, 251-266; d) Revell, J. D.; Wennemers, H. *Curr. Opin. Chem. Biol.* **2007**, *11*, 269-278; e) Hechavarría Fonseca, M.; List. B. *Curr. Opin. Chem. Biol.* **2004**, *8*, 319-326; f) Wennemers, H. Combinatorial Methods for the Discovery of Catalysts. In Highlights in Bioorganic Chemistry; Schmuck, C.; Wennemers, H., Eds.; Wiley-VCH: Weinheim, **2004**, pp. 436-445; g) Berkessel, A. *Curr. Opin. Chem. Biol.* **2003**, *7*, 409-419.

[4] Zhu, J.; Bienyamé, H. *Multicomponent Reactions*; Wiley-VCH, Weinheim, **2005**.

[5] a) Brauch, S.; van Berkel, S. S.; Westermann, B. *Chem. Soc. Rev.* **2013**, *42*, 4948-4962; b) Dömling, A.; Wang, W.; Wang, K. *Chem. Rev.* **2012**, *112*, 3083-3135; c) Ruijter, E.; Scheffelaar, R.; Orru, R. V. A. *Angew. Chem. Int. Ed*. **2011**, *50*, 6234-6246; d) Wessjohann, L. A.; Rivera, D. G.; Vercillo, O. E. *Chem. Rev.* **2009**, *109*, 796-814; e) El Kaïm, L.; Grimaud, L. *Tetrahedron* **2009**, *65*, 2153-2171.

[6] a) Ruijter, E.; Orru, R. V. A. *Drug Discov. Today Technologies* **2013**, *10*, 15-20; b) Slobbe, P.; Ruijter, E.; Orru, R. V. A. *Med. Chem. Commun.* **2012**, *3*, 1189-1218; c) Akritopoulou-Zanze, I. *Curr. Opin. Chem. Biol.* **2008**, *12*, 324-331; d) Hulme, C.; Gore, V. *Curr. Med. Chem.* **2003**, *10*, 51-80.

[7] Touré, B. B.; Hall, D. G. *Chem. Rev.* **2009**, *109*, 4439-4486.

[8] a) Wiesner, M.; Revell, J. D.; Wennemers, H. *Angew. Chem. Int. Ed.* **2008**, *47*, 1871- 1874; b) Wiesner, M.; Revell, J. D.; Tonazzi, S.; Wennemers, H. *J. Am. Chem. Soc.* **2008**, *130*, 5610-5611; c) Wiesner, M.; Neuburger, M.; Wennemers, H. *Chem. Eur. J.* **2009**, *15*, 10103-10109; d) Wiesner, M.; Upert, G.; Angelici, G.; Wennemers, H. *J. Am. Chem. Soc.* **2010**, *132*, 6-7; e) Duschmalé, J.; Wennemers, H. *Chem. Eur. J.* **2012**, *18*, 1111-1120; d) Duschmalé, J.; Wiest, J.; Wiesner, M.; Wennemers, H. *Chem. Sci.* **2013**, *4*, 1312-1318. For similar organocatalyst design, see: f) Ramasastry, S. S. V.; Albertshofer, K.; Utsumi, N.; Barbas III, C. F. *Org. Lett.* **2008**, *10*, 1621-1624. g) Lipshutz, B. H.; Ghorai, S. *Org. Lett.* **2012**, *14*, 422-425. h) Vishnumaya, M. R.; Singh, V. K. *Org. Lett.* **2009**, *74*, 4289-4297. i) Schwab, R. S.; Galetto, F. Z.; Azeredo, J. B.; Braga, A. L.; Ludtke, D, S.; Paixão, M. W. *Tetrahedron Lett.***2008**, *49*, 5094-5097.

[9] a) Revell, J. D.; Gantenbein, D.; Krattiger, P.; Wennemers, H. *Biopolymers* **2006**, *84*, 105-113; b) Revell, J. D.; Wennemers, H. *Tetrahedron* **2007**, *63*, 8420-8424; c) Revell, J. D.; Wennemers, H. *Adv. Synth. Catal.* **2008**, *350*, 1046-1052; d) Messerer, M.; Wennemers, H. *Synlett* **2011**, 499-502.

[10] a) Dömling, A.; Ugi, I. *Angew. Chem., Int. Ed*. **2000**, *39*, 3168-3210; b) Marcaccini, S.; Torroba, T. *Nature Prot.* **2007**, *2*, 632-639; c) Ugi, I.; Meyr, R.; Fetzer, U.; Steinbrücker, C. *Angew. Chem*. **1959**, *71*, 386.

[11] a) Wessjohann, L. A.; Rhoden, C. R. B.; Rivera, D. G.; Vercillo, O. E. *Top. Heterocycl. Chem.* **2010**, *23*, 199-226; b) Gulevich, A. V.; Zhdanko, A. G.; Orru, R. V. A.; Nenajdenko, V. G. *Chem. Rev.* **2010**, *110*, 5235-5331; c) Dömling, A. *Chem. Rev.* **2006**, *106*, 17-89; d) Wessjohann, L. A.; Andrade, C. K. Z.; Vercillo, O. E.; Rivera, D. G. *Targets Heterocycl. Syst.* **2006**, *10*, 24-53; e) Ugi, I.; Marquarding, D.; Urban, R. In *Chemistry and Biochemistry of Amino Acids, Peptides and Proteins*; Weinstein, B., Ed.; Marcel Dekker: New York, **1982**, pp.246-289.

[12] Znabet, A.; Ruijter, E.; de Kanter, F. J. J.; Köhler, V.; Helliwell, M.; Turner, N. J.; Orru, R. V. A. *Angew. Chem. Int. Ed.* **2010**, *49*, 5289-5292.

[13] For examples of peptide-peptoid hybrids, see: a) Rivera, D. G.; León, F.; Concepción, O.; Morales, F. E.; Wessjohann, L. A. *Chem. Eur. J.* **2013**, *19*, 6417-6428; b) Brandt, W.; Herberg, T.; Wessjohann, L. *Biopolymers (Pept. Sci.)* **2011**, *96*, 651-668; c) Olsen, C. A. *ChemBioChem* **2010**, *11*, 152-160; d) Patch, J. A.; Kirshenbaum, K.; Seurynck, S. L.; Zuckermann, R. N.; Barron, A. E. In *Pseudo-peptides in Drug Discovery*; Nielsen, P. E., Ed.; Wiley-VCH: Weinheim, **2004**, pp.1-30.

[14] The multicomponent approach of Orru and co-workers (ref. 12) to a prolyl peptide catalyst encompasses the utilization of only one element of diversity, that is the isocyanide, while *N*-protected D-proline and chiral 1-pyrrolines were used as fixed components. Consequently, such a seminal report may not be regarded as combinatorial.

[15] For selected reviews, see: a) Chowdari, N. S.; Ramachary, D. B.; Barbas, C. F. *Synlett* **2003**, *12*, 1906-1909; b) List, B. *Acc. Chem. Res.* **2004**, *37*, 548-557; c) Dalko, P. I.; Moisan, L. *Angew. Chem. Int. Ed.* **2004**, *43*, 5138-5175; d) Seayad, J.; List, B. *Org. Biomol. Chem.* **2005**, *3*, 719-724; e) Tsogoeva S. B. *Eur. J. Org. Chem.* **2007**, 1701-1716; f) Zhang, Y.; Wang, W. *Catal. Sci. Technol.* **2012**, *2*, 42-53.

[16] a) List, B.; Pojarliev, P.; Martin, H. J. *Org. Lett.* **2001**, *3*, 2423-2425; b) Betancort, J. M.; Barbas, C. F. *Org. Lett.* **2001**, *3*, 3737-3740.

[17] a) Moberg, C. *Angew. Chem. Int. Ed.* **2013**, *52*, 2160-2162; b) Burés, J.; Armstrong, A.; Blackmond, D. G. *J. Am. Chem. Soc.* **2012**, *134*, 6741-6750; c) Seebach, D.; Sun, X.; Sparr, C.; Ebert, M.-O.; Schweizer, W. B.; Beck, A. K. *Helv. Chim. Acta* **2012**, *95*, 1064-1078; d) Patora-Komisarska, K.; Benohoud, M.; Ishikawa, H.; Seebach, D.; Hayashi, Y. *Helv. Chim. Acta* **2011**, *94*, 719-745; e) Burés, J.; Armstrong, A.; Blackmond, D. G. *J. Am. Chem. Soc.* **2011**, *133*, 8822-8825.

[18] Hayashi, Y.; Gotoh, H.; Hayashi, T.; Shoji, M. *Angew. Chem. Int. Ed.* **2005**, *44*, 4212-4215.

[19] This a typical feature of short peptoids and peptide-peptoid hybrids, see for example: Sui, Q.; Borchardt, D.; Rabenstein, D. L. *J. Am. Chem. Soc.* **2007**, *127*, 12042-12048.

[20] Seebach, D.; Golinski, J.; *Helv. Chim. Acta* **1981**, *64*, 1413-1423.

[21] Barros, M. T.; Phillips, A. M. F. *Eur. J. Org. Chem.* **2007**, 178-185.

[22] Cheng, Y.-Q.; Bian, Z.; He, Y.-B.; Han, F.-S.; Kang, C.-Q.; Ning, Z.-L.; Gao, L.-X. *Tetrahedron Asymm.* **2009**, *20*, 1753-1758.

[23] Polak, E.; Ribiere, G. *Revenue Francaise Informat. Recherche Operationelle, Serie Rouge,* **1969**, *16*, 35.

[24] Halgren, T. A. *J. Comput. Chem.* **1996**, *17*, 490-519.

[25] a) MacroModel, version 9.9, Schrödinger, LLC, New York, NY, 2012; b) Richards, N. G. J.; Guida, W. C.; Liskamp, R.; Lipton, M.; Caufield, C.; Chang, G.; Hendrickson, T.; Still, W. C. *J. Comput. Chem.* **1990**, *11*, 440-467.

[26] Maestro, version 9.3, Schrödinger, LLC, New York, NY, 2012.

[27] http://www.schrodinger.com/scriptcenter

[28] a) Manetti, C.; Fogliano, V.; Ritieni, A.; Santini, A.; Randazzo, G.; Logrieco, A.; Mannina, L.; Sagre, A. L. *Structural Chemistry.* **1995**, *6*, 183-189; b) Gouda, H.; Sunazuka, T.; Ui, H.; Handa, M.; Sakoh, Y.; Iwai, Y.; Hirono, A.; Omura, S. *Proc. Natl. Acad. Sci. USA* **2005**, *102*, 18286-18291; c) Shao, J.; Tanner, S. W.; Thompson, N.; Cheatham III, T. E. *J. Chem. Theory. Comput.* **2007**, *3*, 2312-2334.

[29] a) Zhao, Y.; Truhlar, D. G. *Theor. Chem. Acc.* **2008**, *120*, 215-241; b) Zhao, Y. and Truhlar, D. G. *Acc. Chem. Res.* **2008**, *41*, 157-167.

[30] Gaussian 09, Revision B.1, Frisch, M. J.; Trucks, G. W.; Schlegel, H. B.; Scuseria, G. E.; Robb, M. A.; Cheeseman, J. R.; Scalmani, G.; Barone, V.; Mennucci, B.; Petersson, G. A.; Nakatsuji, H.; Caricato, M.; Li, X.; Hratchian, H. P.; Izmaylov, A. F.; Bloino, J.; Zheng, G.; Sonnenberg, J. L.; Hada, M.; Ehara, M.; Toyota, K.; Fukuda, R.; Hasegawa, J.; Ishida, M.; Nakajima, T.; Honda, Y.; Kitao, O.; Nakai, H.; Vreven, T.; Montgomery, Jr., J. A.; Peralta, J. E.; Ogliaro, F.; Bearpark, M.; Heyd, J. J.; Brothers, E.; Kudin, K. N.; Staroverov, V. N.; Kobayashi, R.; Normand, J.; Raghavachari, K.; Rendell, A.; Burant, J. C.; Iyengar, S. S.; Tomasi, J.; Cossi, M.; Rega, N.; Millam, N. J.; Klene, M.; Knox, J. E.; Cross, J. B.; Bakken, V.; Adamo, C.; Jaramillo, J.; Gomperts, R.; Stratmann, R. E.; Yazyev, O.; Austin, A. J.; Cammi, R.; Pomelli, C.; Ochterski, J. W.; Martin, R. L.; Morokuma, K.; Zakrzewski, V. G.; Voth, G. A.; Salvador, P.; Dannenberg, J. J.; Dapprich, S.; Daniels, A. D.; Farkas, Ö.; Foresman, J. B.; Ortiz, J. V.; Cioslowski, J.; Fox, D. J. Gaussian, Inc., Wallingford CT, **2009**.

[31] Marenich, A. V.; Cramer, C. J.; Truhlar, D. G. *J. Phys. Chem. B.* **2009**, *113*, 6378-6396.